Investigation of intramolecular interactions in crystals of Tetrazene explosive and its salts

Maksim A. Samsonov,[a] Jan Ryšavý,[b] Aleš Růžička,[a] Robert Matyáš[b]

[a]Department of General and Inorganic Chemistry, Faculty of Chemical Technology, University of Pardubice, Studentská 573, CZ-532 10, Pardubice, Czech Republic

[b]Institute of Energetic Materials, Faculty of Chemical Technology, University of Pardubice, Studentská 573, CZ-532 10, Pardubice, Czech Republic

KEYWORDS: Tetrazene, Charge density analysis, QTAIM, DFT-calculations

ABSTRACT

In this work, new polymorphic modifications of 1-amino-1-[(1H-tetrazol-5-yl)azo]guanidine hydrate (tetrazene) explosive is presented. The quantum-chemical calculations have been performed in order to estimate the relative energies of tetrazene structural isomers. Five tetrazene salts were prepared by its reactions with mineral acids. High-resolution X-ray diffraction study in 1-amino-1-[(1H-tetrazol-5-yl)azo]guanidinium bromide crystal together with the electron density topology analysis have been carried out. Both experimental and theoretical comparison of all compounds, based on the number and strength of intermolecular contacts, shows strong influence of the solvate and nature of the anion present in compounds supramolecular architecture.

INTRODUCTION

Despite the title substance being in use for more than 100 years[1] and known even longer, many of what is now considered basic information have never been published. This year marks 50 years since the discovery of the correct structure of tetrazene.[2]

Tetrazene is an important industrial primary explosive widely used as an energetic sensitizer in many initiating compositions, particularly in percussion and stab priming mixtures[1, 3] used for the ignition of powder charge in cartridges and initiation devices in other munitions products respectively. Tetrazene was first prepared by Thiele in 1892 by diazotiation of aminoguanidine nitrate with sodium nitrite in the presence of acetic acid.[4] Hofmann and Roth, to whom the discovery of this substance is often incorrectly attributed,[3, 5-9] studied tetrazene in greater detail in 1910.[10] Like there was a certain misattribution regarding the discovery, the view on chemical structure of tetrazene has changed over eight decades. At the beginning, Hofmann and Roth tentatively named this compound as "Amidoguanidin-diazohydroxid"[10] and their proposed structures were "Guanyl-diazoguanyl-tetrazen" (Fig. 1, I) and/or "Guanyl-nitrosoamidoguanyl-tetrazen" (Fig. 1, II).[11] The structure elucidations were developed on elemental analysis results and degradation reaction studies.[11] The azo group in these structures was confirmed by dye-producing coupling reactions[10-12] and utilized in polarographic quantitative analysis later on.[13-15] Based on the presence of four nitrogens in one row in its molecule the compound obtained the acronym "tetrazene" and based on the chemical name of structure (II) it obtained abbreviation GNGT. Both designations are commonly used to present days.

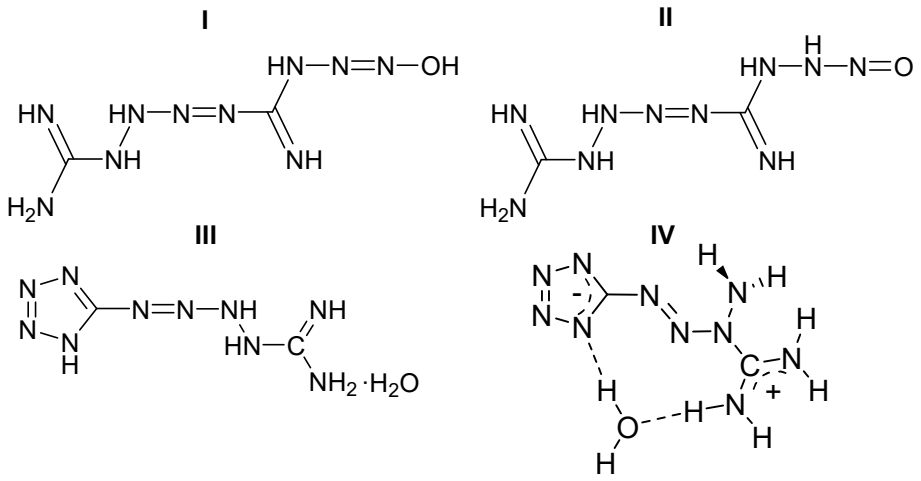

Figure 1. The structures of tetrazene suggested by Hofmann and Roth (I, II) [11], by Patinktin[16] as 4-(1H-tetrazol-5-yl)tetraaz-3-ene-1-carboximidamide hydrate (III), by Duke[2] as 5-[(1E)-3-amidiniotetraz-1-en-1-yl]tetrazolate hydrate (IV).

Toward the end of 1940's and during 1950's studies of ultra-violet absorption spectra hinted at the presence of tetrazole ring,[17-18] which Patinkin et al.[16] confirmed in their revisiting of tetrazene degradation studies and confirmed hydrate water via Karl-Fischer titration, thus proposing a new structure (Fig. 1, III) that was not far from truth.

However, it took until X-ray crystallography methods to fully illuminate the tetrazene structure. Duke[2] revealed the correct position of amino group in the molecule and proved zwitterionic structure of tetrazene molecule (Fig. 1, IV). Duke was also the first to observe the formation of two crystal modifications and designated them as A and B forms.

Considering that the tetrazene molecule is a zwitterion, the N=N bond in the linear part of the molecule is in the E (trans) configuration, the negative charge in tetrazole ring is distributed throughout the ring and the positive charge is evenly distributed in the amidine moiety, the name 5-[(1E)-3-amidiniotetraz-1-en-1-yl]tetrazolate hydrate is the most appropriate. Other commonly used names, such as tetrazolyl guanyltetrazene,[6] 1-amino-1-(tetrazol-5-yldiazenyl)guanidin

monohydrate[3] or 1-amino-1-[(1H-tetrazol-5-yl)azo]guanidine hydrate,[2] disregard the zwitterionic nature of the compound.

This history has led to some confusion and difficulty in tetrazene cataloging – the obsolete structures of tetrazene are still widely used in scientific literature. As a result, one can find tetrazene related articles under each of these structures and corresponding CAS numbers, while missing others because of search results not always overlapping: Both linear structures I and II are found under 109-27-3, Patinkin's structure III is found under 857750-89-1 (monohydrate) and 539-57-1 (anhydrous form) and Duke's structure under 31330-63-9 (monohydrate) and 776249-85-5 (anhydrous form). However, the anhydrous forms are likely the result of machine cataloging and we have found no evidence supporting the existence of such a form. Search engines also recognize the number 89303-69-5 as Duke's structure but it is no longer officially used. Duke's structure (31330-63-9) is expected to be the final and most accurate representation of tetrazene's structure as new groundbreaking discoveries are unlikely.

On top of receiving search results related to other tetrazene moiety containing molecules, the confusion is further amplified when the historic alternate spelling is considered ('tetracene') which leads to problems of the explosive being mistaken for the polycyclic aromatic hydrocarbon of the same name (CAS 92-24-0) and vice versa, thus giving hits for unrelated articles in either direction (example of use of both 'C' and 'Z' spellings in one text[19]).

Tetrazene's zwitterion structure lends itself to the creation of two series of tetrazene salts – anionic and cationic – and although the existence of some of these salts is known, the information is usually limited to the preparation[10-11, 20] and observations such as much more explosive than tetrazene itself[11] or that they are especially interesting.[7-9] Despite this fact, their chemical structure has never been studied and described.

In this article we would like to take a step back to shine further light on the structure of tetrazene and focus on the characterization of its salts.

EXPERIMENTAL SECTION

General Methods

The following methods were used for characterization of powdered (bulk) compounds. Differential thermal analysis was carried out with a DTA 550 Ex thermal analyser produced by OZM Research (Czech Republic). The samples were tested in open glass micro-test tubes in contact with air. The weight of samples was 3–5 mg, the heating rate was 5°C·min^{-1}. Decomposition of tetrazene was accompanied by a strong acoustic effect and the destruction of the micro-test tube.

Elemental analysis was carried out using automatic elemental analyzer UNICUBE (Elementar, Germany) on 1–2 mg samples.

Infrared spectra were collected using a Nicolet iS50 FT-IR spectrometer (Thermo, USA) with an ATR single reflection ZnSe accessory GladiATR (PIKE, USA) and iS50ATR diamond accessory. Measurement parameters were: spectral region 4000–600 cm^{-1} (ZnSe) and 4000–400 cm^{-1} (diamond), resolution 4 cm^{-1} and number of scans 64.

Sensitivity to impact was measured using Kast's fall hammer. Testing sets composed of steel guides BFH-SC and cylinders BFH-SR. Sensitivity to friction was determined using small BAM apparatus type FSA-12. Testing set consisted of porcelain BFST Pt 100 25x25 mm plates and BFST Pn 200 pegs. All sensitivity measurement apparatus and related supplies were manufactured by OZM Research (Czech Republic). Sensitivities to friction and impact were evaluated using probit analysis at 15 trials on each intensity level (at least 5 levels where possible) and results were expressed as a friction force or impact energy with 50% probability of initiation.[21]

Safety Precautions (Robert, I just took it from another article about expl. Materials. Is it ok? Or you would like to correct it?)

Caution! Although we experienced no difficulties in handling these energetic materials, manipulations must be carried out by using standard safety precautions. All compounds should be handled with extreme care, and gloves and eye protection must be worn.

Synthesis and crystallization

Methods of preparation bulk materials for corresponding compound are described in SI with their IR spectrums. Below are the protocols for obtaining single crystals of these compounds.

Single crystalline material ($TZNH^+ \cdot Br^-$, B form)

Tetrazene (0.1 g; 0.53 mmol) was during heating to 40 °C dissolved in as little 48 w.% hydrobromic acid as possible (about 2–5 ml). A test tube was filled with 1 ml of this stock solution and placed into an atmosphere of diethylether in a closed vessel and left undisturbed. In 8–36 hours crystals are formed. The stock solution may be diluted in the test tube with the acid if resulting crystals are unsatisfactory.

Single crystalline material ($TZNH^+ \cdot HSO_4^-$)

Tetrazene (0.1 g) was wetted with few drops of water, followed by addition of enough sulfuric acid (1:1 acid to water by volume; about 15–20 ml) to dissolve the solid to the point of leaving light turbidity. The mixture was heated enough to full dissolution, followed by undisturbed cooling, resulting in crystalline material.

Single crystalline material ($TZN \cdot H_2O$, C form)

Sodium nitrite (6 g; 87.0 mmol) and bisaminoguanidinium sulfate (7 g; 28.4 mmol) were dissolved in water (100 ml). Acetic acid was used to adjust the pH to the initial value range of 5.2–5.7. The mixture was then left undisturbed at laboratory temperature. The following day large

orange-yellow needles were found. The mixture remains active and after a week further product can be obtained, yielding 3.5 g (70.7 %) of product.

Single crystalline material ($TZNH^+ \cdot Cl^-$, $TZNH^+ \cdot ClO_4^-$, $TZN \cdot H_3PO_4$)

The procedure for tetrazene bromide was used for tetrazene chloride, tetrazene perchlorate and tetrazene phosphate.

X-ray Crystallography

Full-sets of diffraction data for all of compaunds were collected at 150(2)K with a Bruker D8-Venture diffractometer equipped with Mo (Mo/Kα radiation; λ = 0.71073 Å) microfocus X-ray (IμS) source, Photon CMOS detector and Oxford Cryosystems cooling device was used for data collection. The frames were integrated with the Bruker SAINT software package using a narrowframe algorithm. Data were corrected for absorption effects using the Multi-Scan method (SADABS). Obtained data were treated by XT-version 2014/5 and SHELXL-2014/7 software implemented in APEX3 v2018.1-0 (Bruker AXS) system.[22] Hydrogen atoms were localized on a difference Fourier map.

The multipole refinement was carried out within the Hansen–Coppens formalism[23] using the MoPro program package.[24] Before the refinement, C–H bond distances were normalized to the values obtained in neutron diffraction analyses.[25] The level of the multipole expansion was hexadecapole for the Br1, octupole for all other non-hydrogen atoms, and one dipole for hydrogen atoms. The refinement of compound $^{ED}TZNH^+ \cdot Br^-$ was carried out against F and converged to R = 0.0626, wR = 0.0495, GOF = 1.324 for 9817 merged reflections with $I>2\sigma(I)$. All bonded pairs of atoms satisfy the Hirshfeld rigid-bond criteria.[26] Analysis of topology of the experimental $\rho(r)$ function was carried out using the MoProViewer program.[27] The residual electron densities around

Br is 1.75e, however, attempts to reduce this value by varying the parameters when taking absorption into account have not been successful.

Crystallographic data for structural analysis have been deposited with the Cambridge Crystallographic Data Centre, CCDC nos. xxxxx-xxxxxx. Copies of this information may be obtained free of charge from The Director, CCDC, 12 Union Road, Cambridge CB2 1EY, UK (fax: +44-1223-336033; e-mail: deposit@ccdc.cam.ac.uk or www: http://www.ccdc.cam.ac.uk).

DFT-calculations and QTAIM analysis

Theoretical Calculations. All the calculations were performed with the Gaussian 16 program.[28] The different geometries of tetrazene were fully optimised at the B3LYP-D3/6-311++G(d,p) level of theory.[29-31] All the computed structures are minima on the potential energy surface, as confirmed by the frequency calculations at the same level of theory. Relative energies were estimated as the difference between the energy of the state obtained from X-ray data and the and other possible structures, including zero-point energies (ZPEs). To estimate of intermolecular interactions around tetrazene molecule further arranged nearest neighbouring molecules. Clusters were calculated at the same level of theory, all of non-Hydrogen atoms were fixed. The topological analysis of the theoretical function $\rho(r)$ was performed using the AIMALL program package.[32]

RESULTS AND DISCUSSION

As noted above, the crystal structure of tetrazene was established 50 years ago,[2] but there is still no unified opinion of the position of the H atoms in the molecule. For example, on various open resources such as: PubChem.com, commonchemistry.cas.org, Wikipedia.org, the structural formulae differ. To clarify this point, the corresponding DFT-calculations were performed and the relative energies of each of the possible structures of free tetrazene *in vacuo* were compared. As can be seen from Fig. 2. The most energetically favorable structure for free tetrazene (molecule

without solvate) is the structure with hydrogen atoms localized in the positions 8- and 4-. At the same time, the position of the H atom at any nitrogen atom in the tetrazole ring is also more energetically favorable, in comparison with the 8, 8-positions found crystallographically for tetrazene hydrate. It should be noted that the calculations were carried out for isolated molecules, therefore, the situation in a crystal / solution may differ significantly. Nevertheless, according to the obtained energies, such transitions can be realized.

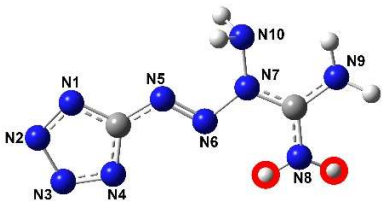

8, 8 position (x-ray*) / 0

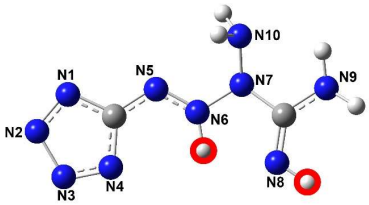

8, 6 position / 11.86

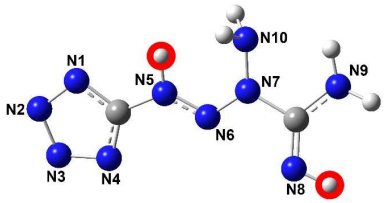

8, 5 position / 22.50

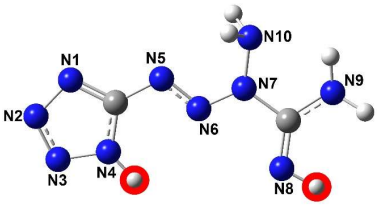

8, 4 position / -12.39

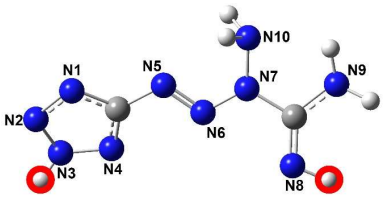

8, 3 position / -10.03

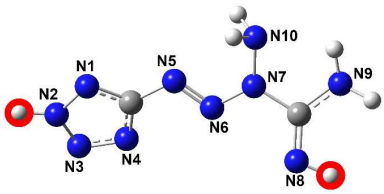

8, 2 position / -9.78

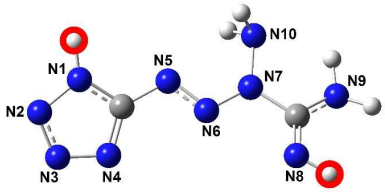

8, 1 position / -8.06

Figure 2. Relative energy (kcal/mol) for structures of tetrazene with different positions of H atoms (red) at the B3LYP-D3/6-311++g(d,p) level of calculations. *X-ray structure of tetrazene hydrate.

The structures and main geometrical parameters of tetrazene hydrate and tetrazene hydrobromide were published in work by Duke, [2] but no detailed study of intermolecular contacts has been carried out. To fill this gap, we conducted the X-ray structural study of 1-amino-1-[(1H-

tetrazol-5-yl)azo]guanidine hydrate (**TZN·H₂O**) and 1-amino-1-[(1H-tetrazol-5-yl)azo]guanidinium bromide (**TZNH⁺·Br⁻**). Surprisingly, the space groups and some unit cell parameters in our experiments differ significantly (Table S4). All attempts to refine it with the same parameters as in the work[2] led to worse final results. Thus, we assume that two new polymorphs **TZN·H₂O** (C-Tetrazene) and **TZNH⁺·Br⁻** (B-Tetrazene hydrobromide) were obtained. Moreover, the **TZNH⁺·Br⁻** crystals were of sufficiently quality, which allowed us to carry out a high-resolution X-ray diffraction study (**^{ED}TZNH⁺·Br⁻**). Structures and main geometrical parameters of **TZN·H₂O** and **TZNH⁺·Br⁻** are shown on Fig. 3 and 4 respectively.

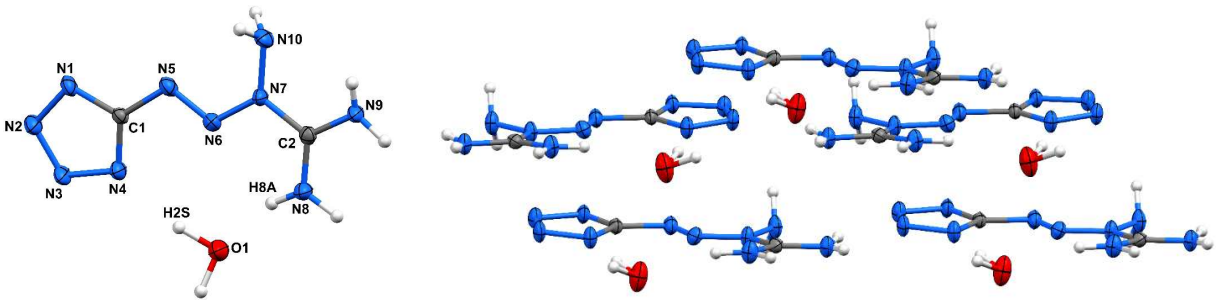

Figure 3. Molecular structures of **TZN·H₂O** and fragment of crystal packing. ORTEP diagram, 50% probability level, selected interatomic distances [Å] and bond angles [°]: N(1)-C(1) 1.344(6), N(1)-N(2) 1.338(4), N(2)-N(3) 1.321(4), N(3)-N(4) 1.344(4), C(1)-N(4) 1.320(5), C(1)-N(5) 1.414(4), N(5)-N(6) 1.266(5), N(7)-N(6) 1.351(4), N(7)-N(10) 1.405(4), C(2)-N(7) 1.385(4), C(2)-N(8) 1.312(5), C(2)-N(9) 1.311(5), N4...H2S 1.88(5), O1...H8A 2.11(5); N(6)-N(5)-C(1) 109.8(3), N(9)-C(2)-N(7), N(9)-C(2)-N(8).

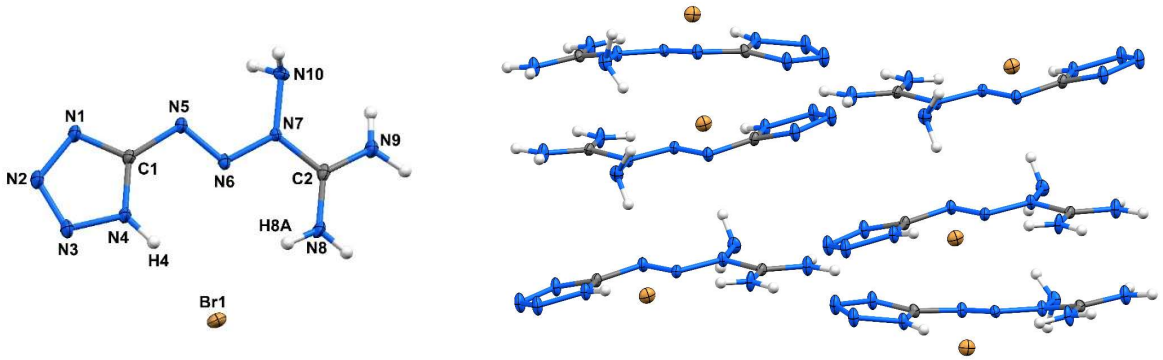

Figure 4. Molecular structures of **TZNH$^+$·Br$^-$** and fragment of crystal packing. ORTEP diagram, 50% probability level, selected interatomic distances [Å] and bond angles [°]: N(1)-C(1) 1.320(2), N(1)-N(2) 1.361(2), N(2)-N(3) 1.299(2), N(3)-N(4) 1.339(2), C(1)-N(4) 1.341(2), C(1)-N(5) 1.398(2), N(5)-N(6) 1.2656(19), N(7)-N(6) 1.3384(19), N(7)-N(10) 1.3940(18), C(2)-N(7) 1.385(2), C(2)-N(8) 1.314(2), C(2)-N(9) 1.308(2), Br1…H4 2.25(3), Br1…H8A 2.57(2); N(6)-N(5)-C(1) 109.42(13), N(9)-C(2)-N(7) 117.35(15), N(9)-C(2)-N(8) 124.17(16).

To quantify the energy of the intermolecular interactions, a precision X-ray diffraction analysis of crystals of **^{ED}TZNH$^+$·Br$^-$** with multipole refinement was carried out. After that, a topological analysis of the experimental electron density based on the quantum theory of atoms in molecules (QTAIM)[33] was performed. The energies of intermolecular interactions were calculated from the Espinosa's equation $E_{int} = 1/2V(r_{cp})$.[34]

The static deformation electron density distribution maps for the guanidine fragment (N10-C2-N9) and tetrazole ring (N4-C1-N1) are presented on Fig. 5. As expected, there is an accumulation of the electron density on the covalent bonds C-N, N-N, in addition, the lone electron pairs (LP) of nitrogen atoms in the tetrazole ring are clearly visible from the figure.

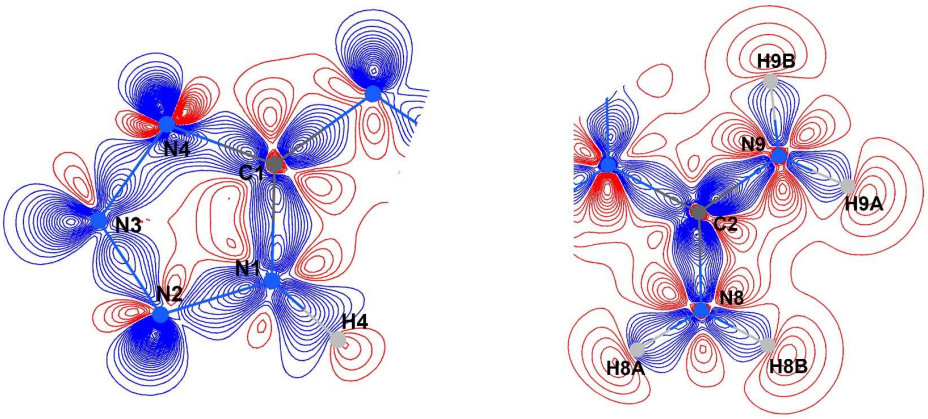

Figure 5. The static deformation electron density distribution in ^{ED}**TZNH**$^{+}$**·Br**$^{-}$: N1-C1-N4 (left) and N9-C2-N8 (right) plates. The positive (blue) and negative (red) contours are drawn at intervals 0.05 e/Å^3.

The molecular graph of ^{ED}**TZNH**$^{+}$**·Br**$^{-}$ demonstrates the presence of bond critical points (3, -1) (BCP) between Br1^{-} and H4, H8A atoms (Fig. 6). In order to identify all intermolecular interactions per one protonated tetrazene molecule, we examined a small fragment of the crystal packing (Fig. 6). In total, 25 BCPs (3, -1) were localized, which include N…H, N…N, Br…H, Br…N and H…H interactions (Table 1). As can be seen from the data in Table. 1 the total energy of all interactions per one molecule is -58.41 kcal/mol, while Br1^{-} anions contribute is -27.12 kcal/mol. All detected interactions can be classified as closed shell interactions.

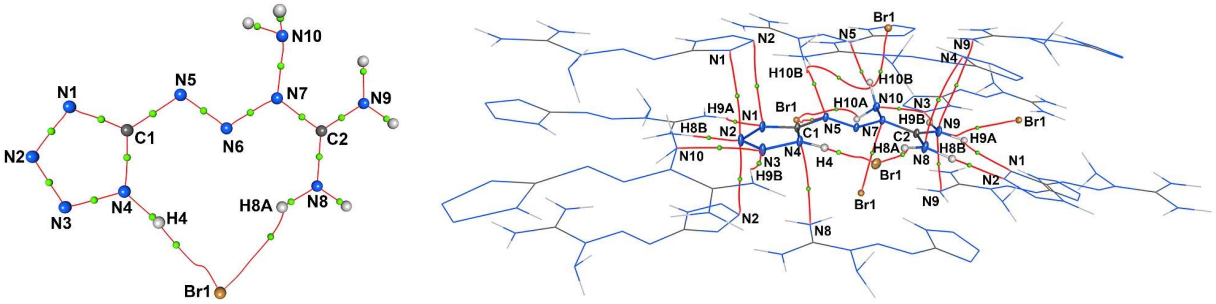

Figure 6. Molecular graph of ^{ED}**TZNH^{+}·Br^{-}** (left) and fragment of the crystal packing (right, atoms participating in intermolecular interactions are signed, BCPs (3, -1) corresponding to these interactions are marked green). Only BCPs (3, -1) are presented for clarity.

We performed the corresponding DFT calculations at the B3LYP-D3/6-311++g(d,p) level of theory for small cluster containing 9 molecules (Fig. 7) to estimate the energy of intermolecular interactions in **TZNH^{+}·Br^{-}** theoretically. The total number of intermolecular contacts is 22, which is somewhat less in comparison with experiment (25). In the case of **TZNH^{+}·Br^{-}**, the total energy of intermolecular interactions was -56.82 kcal/mol, which at first look is very close to the value from the experiment (-58.41 kcal/mol).

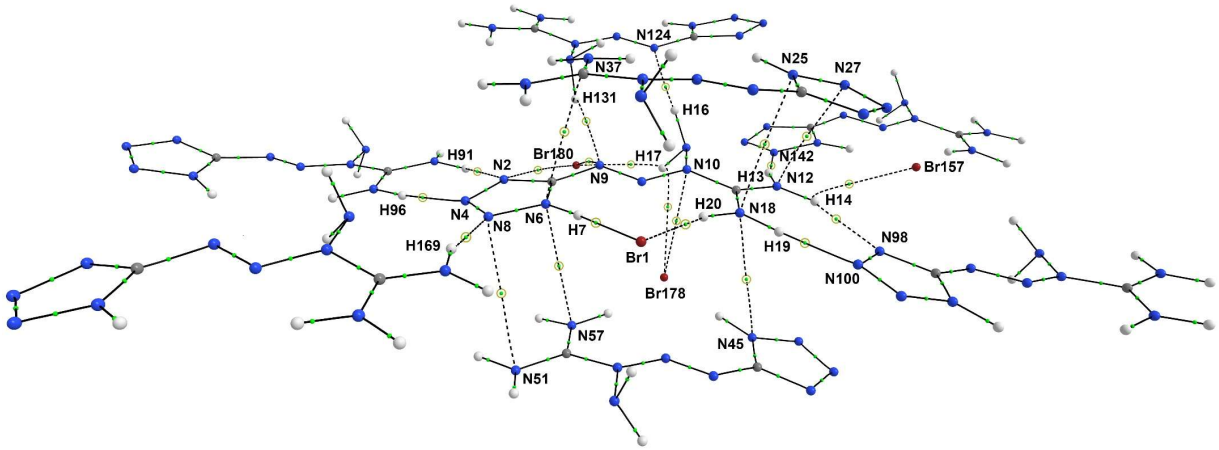

Fig. 7. Fragment of crystal packing of **TZNH^{+}·Br^{-}**. Atoms participating in intermolecular interactions are signed, BCPs (3, -1) corresponding to these interactions are marked with a yellow circle. Molecules and anions not participating in intermolecular interaction with the central molecule are not shown for clarity.

However, a detailed analysis of topological parameters (Table 1) shows that theoretical calculations somewhat overestimate N…H and underestimate N…Br, H…Br interactions. Thus, the sum of all intermolecular interactions tends to the experimental value. The main intermolecular

contacts found in **TZNH$^+$·Br$^-$** correspond to those in **^{ED}TZNH$^+$·Br$^-$** (Table 1), however, some differences are observed, probably due to different curvature of the electron density obtained as a result of the experiment and theoretically. Similar calculations were carried out for **TZN·H$_2$O** (Fig. S4, Table S5). 21 intermolecular contacts were found with E_{int} equals to -72.77 kcal/mol. However, when a possibility of forming intermolecular contacts due to the OH group appears, the solvent contribution is -3.2 kcal/mol more in comparison with **TZNH$^+$·Br$^-$**.

Table 1. Topological properties of BCPs (3, -1) in **^{ED}TZNH$^+$·Br$^-$ / TZNH$^+$·Br$^-$** (theory) (a.u.) and energies of intermolecular interactions E_{int} (kcal/mol), values in brackets correspond to theoretical data.*

Experimental data						
Atom 1	Atom 2	$\rho(r_{cp})$	$\nabla^2\rho(r_{cp})$	$G(r_{cp})$	$V(r_{cp})$	E_{int}
Br1	H4	0.299	2.505	0.033	-0.041	-12.7
Br1	N7	0.104	1.041	0.010	-0.009	-2.8
Br1	N9	0.032	0.329	0.003	-0.002	-0.6
N5	Br1	0.062	0.663	0.006	-0.005	-1.4
H10B	Br1	0.109	1.060	0.010	-0.010	-3.0
H10A	Br1	0.063	0.892	0.007	-0.005	-1.7
Br1	H8A	0.136	1.914	0.018	-0.015	-4.8
N4	N8	0.034	0.423	0.003	-0.002	-0.7
N1	N2	0.040	0.575	0.005	-0.003	-1.0
N2	N2	0.024	0.354	0.003	-0.002	-0.5
N8	N4	0.034	0.423	0.003	-0.002	-0.7
N2	N1	0.040	0.575	0.005	-0.003	-1.0
N3	N10	0.029	0.457	0.004	-0.002	-0.7

N10	N3	0.029	0.459	0.004	-0.002	-0.7
N9	N9	0.009	0.121	0.001	-0.001	-0.2
N9	N9	0.009	0.121	0.001	-0.001	-0.2
N2	H8B	0.139	3.327	0.027	-0.020	-6.4
N1	H9A	0.064	1.296	0.010	-0.007	-2.2
N3	H9B	0.059	1.421	0.011	-0.007	-2.2
H9B	N3	0.059	1.422	0.011	-0.007	-2.2
H8B	N2	0.139	3.327	0.027	-0.020	-6.4
N5	H10B	0.055	1.034	0.008	-0.005	-1.7
H10B	N5	0.055	1.034	0.008	-0.005	-1.7
H9A	N1	0.064	1.296	0.010	-0.007	-2.2
Theoretical data						
Atom 1	Atom 2	$\rho(\boldsymbol{r}_{cp})$	$\nabla^2\rho(\boldsymbol{r}_{cp})$	$G(\boldsymbol{r}_{cp})$	$V(\boldsymbol{r}_{cp})$	E_{int}
N2	H91	0.015	0.052	0.011	-0.009	-2.69
N4	H96	0.033	0.102	0.026	-0.026	-8.24
N8	H169	0.015	0.054	0.011	-0.009	-2.70
H13	N142	0.016	0.053	0.011	-0.008	-2.64
N9	H131	0.012	0.040	0.008	-0.007	-2.09
H14	N98	0.016	0.054	0.011	-0.009	-2.87
H19	N100	0.034	0.099	0.026	-0.027	-8.43
H16	N124	0.014	0.046	0.010	-0.008	-2.42
N18	N25	0.006	0.016	0.004	-0.003	-0.97
N12	N27	0.004	0.011	0.002	-0.002	-0.62
N6	N37	0.004	0.013	0.003	-0.002	-0.74
N18	N45	0.004	0.012	0.003	-0.002	-0.72
N8	N51	0.004	0.012	0.003	-0.002	-0.66

N6	N57	0.005	0.016	0.003	-0.003	-0.94
Br1	H7	0.043	0.057	0.023	-0.032	-9.99
H17	Br178	0.008	0.026	0.005	-0.004	-1.36
H17	Br180	0.010	0.025	0.005	-0.004	-1.31
Br1	H20	0.020	0.052	0.012	-0.011	-3.53
H14	Br157	0.003	0.009	0.002	-0.001	-0.38
N10	Br178	0.010	0.030	0.007	-0.006	-1.80
N2	Br180	0.004	0.009	0.002	-0.002	-0.47
N9	Br180	0.008	0.023	0.005	-0.004	-1.24

*$\rho(r_{cp})$ - the electron density, $\nabla^2\rho(r_{cp})$ - the Laplacian function of the electron density, $G(r_{cp})$ - the kinetic electron energy density, $V(r_{cp})$ - the potential electron energy density.

In order to investigate the nature of the solvent and its influence on the packing motifs as well as energies of intermolecular contacts, we obtained a series of crystals with different solvent molecules/anions: **TZNH$^+$·Cl$^-$**, **TZNH$^+$·ClO$_4^-$**, **TZN·HSO$_4^-$**, **TZN·H$_3$PO$_4$**. Geometry analysis showed that the tetrazene molecule in the protonated form is approximately flat, however, depending on the nature of the neighboring molecules (solvent molecule / anion) and the packing characteristics, the angles between the planes of the tetrazole ring (C1-N4) and the guanidine fragment (C2, N7- N9) can vary over a wide range of 6.09-17.9° (Table S1). The greatest distortions are observed in cases **TZNH$^+$·Br** (17.9°) and **TZNH$^+$·Cl$^-$** (16.74°), while the smallest distortions are observed in **TZNH$^+$·HSO$_4^-$** (6.15°) and **TZN·H$_2$O** (6.09°), respectively. The main bond lengths in all crystals have similar values, differences are observed for N2-N3 bonds (Table S2) in protonated forms, they vary in the range 1.296(3)-1.299(2) Å, while for **TZN·H$_2$O**, **TZN·H$_3$PO$_4$** it is 1.3127(14) -1.344(4) Å, respectively.

Packing motifs in the crystals are presented in the form of parallel layers, but in packing of **TZN·HSO$_4$** there are also layers oriented perpendicularly (Fig. 3, 4, 8, S1,S2). Analysis of packing motifs revealed the presence of a large number of intermolecular short contacts. The number of such contacts per one tetrazene molecule varies from 13 in **TZNH$^+$·Br$^-$** to 22 in **TZN·H$_3$PO$_4$** respectively (Table S3).

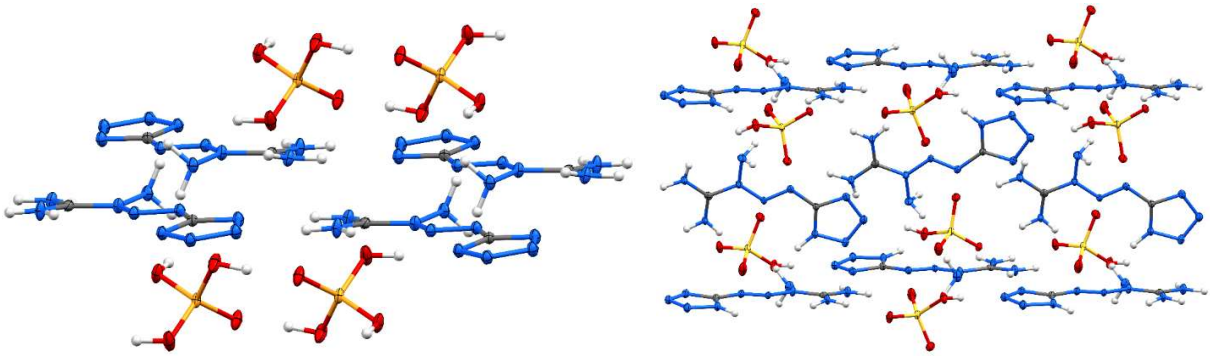

Fig. 8. Fragments of crystal packing in **TZN·HSO$_4^-$** (left) and **TZN·H$_3$PO$_4$** (right). ORTEP diagram, 50% probability.

The topological parameters for the series are presented in Tables S5-9. The values of intermolecular contacts vary for **TZNH$^+$·Br$^-$**–**TZN·H$_2$O** crystals in the range -0.2 to -25.11 kcal/mol. The value of -25.11 kcal/mol corresponds to the O-H6...N9 interaction in **TZN·H$_3$PO$_4$** (Fig. S8, Table S9). The H6...N9 distance is the shortest intermolecular contact among the crystals and is 1.67(3)/[1.5483] Å in the crystal/calculation, respectively. Such a strong interaction is probably due to the nature of the acid - in the case of a stronger sulfuric acid **TZN·HSO$_4^-$**, we observe a protonated form, while in the case of a weaker orthophosphoric acid, this process is incomplete. It should be noted that in **TZNH$^+$·Br$^-$** and **TZNH$^+$·Cl$^-$** with the same number of intermolecular contacts (22), but the difference in the total E_{int} is -10.97 kcal/mol. The largest number of intermolecular contacts 26 was found in **TZNH$^+$·ClO$_4^-$**, while the total E_{int} is comparable to **TZN·H$_2$O** where the tetrazene molecule is not protonated. Table 3 shows the

contributions of solvents/anions per the molecule. As can be seen from the data in Table 3, the largest contributions are realized for sterically bulky particles capable of forming both O...N and H...N interactions.

Table 3. The total energy of intermolecular interactions obtained theoretically for the series per one molecule of tetrazene (kcal/mol).

Compound	Number of intermolecular interactions	Total E_{int}	Contribution of Anions/solvents
TZN·H_2O	21	-72.77	-24.00
^{ED}TZNH$^+$·Br$^-$	25	-58.41	-27.12
TZNH$^+$·Br$^-$	22	-56.82	-20.08
TZNH$^+$·Cl$^-$	22	-67.79	-26.79
TZNH$^+$·ClO_4^-	26	-71.44	-34.37
TZNH$^+$·HSO_4^-	21	-77.90	-46.94
TZN·H_3PO_4	25	-93.22	-46.46

Explosive properties

Tetrazene itself and its salts are primary explosives. The sensitivity of the explosives to impact and friction are one of the basic sensitivity parameters for primary explosives related to handling safely.

We are aware, finding a relationship between the energy of the intermolecular interactions and sensitivity parameters of studied compounds is quite problematic, since the sensitivity of explosives is tested on powdered samples, but our investigation is made on a single crystalline material. The characteristics of explosives depend not only on the chemical structure, but mainly on the size and shape of crystals and on the content of inhomogeneities (crystal lattice defects, cracks, presence of air pores). Impact or friction then produces hot spots (places with high

temperature) in these inhomogeneities where the detonation process starts.[Please some references about Impact energy and Friction force for understanding what is it]

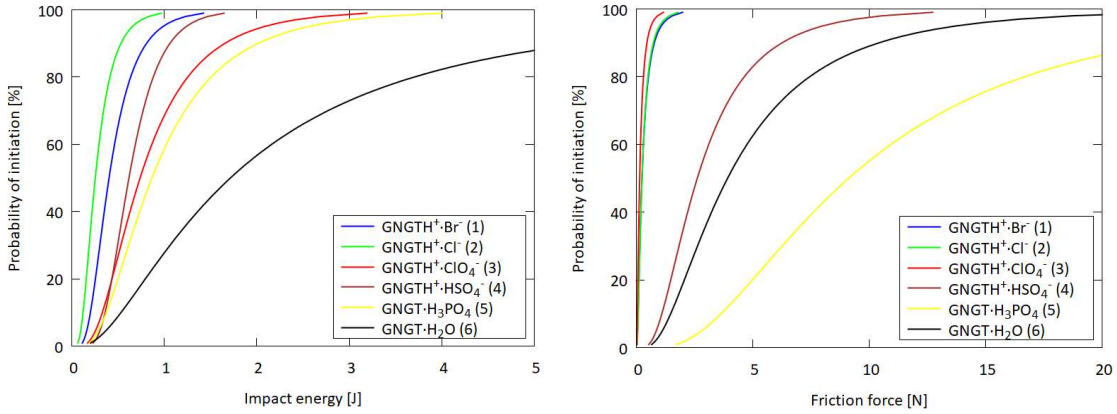

Figure 9. Sensitivity curves of tetrazene and its salts (impact sensitivity, left) and (friction sensitivity, right).

Table 4. Parameters of sensitivity curves.

Compound	Impact sensitivity curves parameters		Friction sensitivity curves parameters	
	Mean μ	Standard deviation σ	Mean μ	Standard deviation σ
$TZNH^+ \cdot Br^-$	-0.8556	0.5349	-1.3435	0.8667
$TZNH^+ \cdot Cl^-$	-1.3920	0.5636	-1.4855	0.8613
$TZNH^+ \cdot ClO_4^-$	-0.2961	0.6262	-1.9236	0.8914
$TZNH^+ \cdot HSO_4^-$	-0.4782	0.4813	0.9559	0.6839
$TZN \cdot H_3PO_4$	-0.1569	0.6849	2.2256	0.7164
$TZN \cdot H_2O$	0.5506	0.9321	1.3863	0.7718

On the other hand, we present here the dependence of probability of initiation on impact energy for studied compounds (Fig.9 left) and the dependence of probability of initiation on friction force (Fig.9 right) in order make a parallel of practical tests and purely academic research on single

crystalline material. Table 4 summarizes the parameters of sensitivity curves. Values of 50 % activation probability of studied compounds are presented in Table 5.

Table 5. Impact (J) and friction (N) sensitivity of tetrazene and its salts.

Compound	Impact energy for 50% probability of initiation	Friction force for 50% probability of initiation
$TZNH^+ \cdot Br^-$	0.43	0.26
$TZNH^+ \cdot Cl^-$	0.25	0.23
$TZNH^+ \cdot ClO_4^-$	0.74	0.15
$TZNH^+ \cdot HSO_4^-$	0.62	2.60
$TZN \cdot H_3PO_4$	0.85	9.26
$TZN \cdot H_2O$	1.73	4.00

In the case of impact sensitivity, all tetrazene salts are significantly more sensitive than tetrazene itself. A similar trend was found for friction sensitivity (except for tetrazene phosphate). The reason for the higher sensitivity of tetrazene salts compared to tetrazene is the absence of a solvent. In general, the presence of water in explosives (whether liquid or in the form of crystal water) reduces the sensitivity of explosives to external stimuli. The least sensitive sample of the tetrazene salts series is its co-crystal with phosphoric acid (especially to friction), which could be seen as a solvate.

CONCLUSIONS

As a result of the study, four new crystals of tetrazene with different solvent molecules / anions were obtained, in addition, for the previously known 1-amino-1-[(1H-tetrazol-5-yl)azo]guanidine hydrate and 1-amino-1-[(1H-tetrazol-5-yl)azo]guanidinium bromide two new polymorphic modifications were discovered. It was shown theoretically that the most energetically favorable structure is tetrazene with 8.4- positions of hydrogen atoms. Precision X-ray structural study has

been carried out in the crystal of tetrazene hydrobromide. For the entire series of crystals, theoretical calculations were carried out, followed by a topological analysis of the electron density. It was investigated how the nature of the solvate molecule / anion affects the amount and value of the energy of intermolecular contacts in tetrazene crystals. The data obtained theoretically with experimental data are compared; it is shown that such an approach gives reasonable values but some interactions can be over-/ underestimated. The data about impact sensitivity for tetrazene and its salts is present.

ASSOCIATED CONTENT

Supporting Information

X-ray structures, crystallographic data, QTAIM data, xyz-file for all calculated structures, cif-file from multipole refinement.

AUTHOR INFORMATION

Corresponding Author

Maksim A. Samsonov - Department of General and Inorganic Chemistry, Faculty of Chemical Technology, University of Pardubice, Studentská 573, CZ-532 10, Pardubice, Czech Republic; https://orcid.org/0000-0002-3839-5939; E-mail: MaksimAndreevich.Samsonov@upce.cz

Author Contributions

The manuscript was written through contributions of all authors. All authors have given approval to the final version of the manuscript.

Funding Sources

Any funds used to support the research of the manuscript should be placed here (per journal style).

ACKNOWLEDGMENT

Thanks everyone.

REFERENCES:

1. Hagel, R.; Redecker, K., Sintox – A New, Non-Toxic Primer Composition by Dynamit Nobel AG. *Propellants, Explos., Pyrotech.* **1986,** *11* (6), 184–187.
2. Duke, J. R. C., *X*-Ray Crystal and Molecular Structure of 'Tetrazene', ('Tetracene'), $C_2H_8N_{10}O$. *J. Chem. Soc. D* **1971,** (1), 2–3.
3. Matyáš, R.; Pachman, J., *Primary Explosives*. Springer: Heidelberg, 2013.
4. Thiele, J., Ueber Nitro- und Amidoguanidin. *Justus Liebigs Ann. Chem.* **1892,** *270* (1–2), 1–63.
5. Agrawal, J. P., *High Energy Materials: Propellants, Explosives and Pyrotechnics*. Wiley-VCH Verlag GmbH & Co. KGaA Weinheim, 2010.
6. Akhavan, J., *The Chemistry of Explosives*. 2nd ed.; The Royal Society of Chemistry: Cambridge, 2004.
7. Davis, T. L., *The Chemistry of Powder and Explosives*. 1941.
8. Fedoroff, B. T.; Aaronson, H. A.; Reese, E. F.; Sheffield, O. E.; Clift, G. D., *Encyclopedia of Explosives and Related Items*. Picatinny Arsenal: New Jersey, 1960.
9. Urbański, T., *Chemie a technologie výbušin*. Státní nakladatelství technické literatury: Praha, 1959; Vol. 3.
10. Hofmann, K. A.; Roth, R., Aliphatische Diazosalze. *Ber. Dtsch. Chem. Ges.* **1910,** *43* (1), 682–688.
11. Hofmann, K. A.; Hock, H.; Roth, R., Diazoverbindungen aus Amidoguanidin, Beiträge zur Kenntnis der Diazohydrazoverbindungen (Tetrazene). *Ber. Dtsch. Chem. Ges.* **1910,** *43* (1), 1087–1095.
12. Shreve, R. N.; Carter, R. P.; Willis, J. M., Azo Dyes from Aminoguanidine. *Industrial and Engineering Chemistry* **1944,** *36* (5), 426–430.
13. Flack, J., Beitrag zur quantitativen Analyse von Tetrazen in Zündsätzen. Polarographische Bestimmung am einzelnen Zündhütchen. *Sprengstoffe und Pyrotechnik* **1973,** *9* (5), 18–22.
14. Flack, J., Quantitative Analysis of Tetracene in Primer Mixtures. Polarographic Determination in Individual Primer Caps. *HSI, Hung. Sci. Instrum.* **1974,** *31*, 17–19.
15. Wild, A. M., Polarographic Estimation of Tetracene. *Chemistry and Industry* **1957**, 1543.
16. Patinkin, S. H.; Horwitz, J. P.; Lieber, E., The Structure of Tetracene. *J. Am. Chem. Soc.* **1955,** *77*, 562–567.
17. Conduit, C. P. *The Ultra-Violet Spectroscopic Examination of Tetrazene*; AD-083780; Ministry of Supply: Waltham Abbey, 1955.
18. Von Hofsommer, R.; Pestemer, M., Über die Ultraviolett-Absorption und Konstitution von Tetrazenen aus Aminoguanidinsalzen. *Z. Elektrochem. Angew. Phys. Chem.* **1949,** *53* (6), 383-387.
19. Fair, H. D.; Walker, R. F., *Energetic Materials 2: Technology of the Inorganic Azides*. Plenum Press: New York, 1977.

20. Hofmann, K. A.; Hock, H.; Kirmreuther, H., Einwirkung von salpetriger Säure auf Amidoguanidin und Semicarbazid; Unterschied zwischen dem Tetrazen $C_2N_{10}H_8O$ und den Aziden im Verhalten gegen Jodwasserstoffsäure *Justus Liebigs Ann. Chem.* **1911,** *380* (2), 131–147.
21. Šelešovský, J.; Pachmáň, J., Probit Analysis – a Promising Tool for Evaluation of Explosives Sensitivity. *Cent. Eur. J. Energ. Mater.* **2010,** *7* (3), 269–278.
22. *APEX3 v2018.1-0 (Bruker AXS)*.
23. Hansen, N. K.; Coppens, P., Testing aspherical atom refinements on small-molecule data sets. *Acta Crystallographica Section A* **1978,** *34* (6), 909-921.
24. Jelsch, C.; Guillot, B.; Lagoutte, A.; Lecomte, C., Advances in protein and small-molecule charge-density refinement methods using MoPro. *J. Appl. Crystallogr.* **2005,** *38* (1), 38-54.
25. Allen, F. H.; Bruno, I. J., Bond lengths in organic and metal-organic compounds revisited: X-H bond lengths from neutron diffraction data. *Acta Crystallographica Section B* **2010,** *66* (3), 380-386.
26. Hirshfeld, F., Can X-ray data distinguish bonding effects from vibrational smearing? *Acta Crystallographica Section A* **1976,** *32* (2), 239-244.
27. Guillot, B., MoProViewer: a molecule viewer for the MoPro charge-density analysis program. *Acta Crystallographica Section A* **2012,** *68* (a1), s204.
28. Frisch, M. J.; Trucks, G. W.; Schlegel, H. B.; Scuseria, G. E.; Robb, M. A.; Cheeseman, J. R.; Scalmani, G.; Barone, V.; Petersson, G. A.; Nakatsuji, H.; Li, X.; Caricato, M.; Marenich, A. V.; Bloino, J.; Janesko, B. G.; Gomperts, R.; Mennucci, B.; Hratchian, H. P.; Ortiz, J. V.; Izmaylov, A. F.; Sonnenberg, J. L.; Williams; Ding, F.; Lipparini, F.; Egidi, F.; Goings, J.; Peng, B.; Petrone, A.; Henderson, T.; Ranasinghe, D.; Zakrzewski, V. G.; Gao, J.; Rega, N.; Zheng, G.; Liang, W.; Hada, M.; Ehara, M.; Toyota, K.; Fukuda, R.; Hasegawa, J.; Ishida, M.; Nakajima, T.; Honda, Y.; Kitao, O.; Nakai, H.; Vreven, T.; Throssell, K.; Montgomery Jr., J. A.; Peralta, J. E.; Ogliaro, F.; Bearpark, M. J.; Heyd, J. J.; Brothers, E. N.; Kudin, K. N.; Staroverov, V. N.; Keith, T. A.; Kobayashi, R.; Normand, J.; Raghavachari, K.; Rendell, A. P.; Burant, J. C.; Iyengar, S. S.; Tomasi, J.; Cossi, M.; Millam, J. M.; Klene, M.; Adamo, C.; Cammi, R.; Ochterski, J. W.; Martin, R. L.; Morokuma, K.; Farkas, O.; Foresman, J. B.; Fox, D. J. *Gaussian 16 Rev. C.01*, Wallingford, CT, 2016.
29. Becke, A. D., Density-functional thermochemistry. III. The role of exact exchange. *The Journal of Chemical Physics* **1993,** *98* (7), 5648-5652.
30. Grimme, S.; Antony, J.; Ehrlich, S.; Krieg, H., A consistent and accurate ab initio parametrization of density functional dispersion correction (DFT-D) for the 94 elements H-Pu. *The Journal of Chemical Physics* **2010,** *132* (15), 154104.
31. Krishnan, R.; Binkley, J. S.; Seeger, R.; Pople, J. A., Self-consistent molecular orbital methods. XX. A basis set for correlated wave functions. *The Journal of Chemical Physics* **1980,** *72* (1), 650-654.
32. AIMAll (Version 19.10.12), T. A. K., TK Gristmill Software, Overland Park KS, USA, 2019 (aim.tkgristmill.com).
33. Bader, R. F. W., *Atoms in molecules : a quantum theory*. Clarendon Press: Oxford, 1990.
34. Espinosa, E.; Molins, E.; Lecomte, C., Hydrogen bond strengths revealed by topological analyses of experimentally observed electron densities. *Chem. Phys. Lett.* **1998,** *285* (3), 170-173.